Dalton Transactions

Accepted Manuscript

This article can be cited before page numbers have been issued, to do this please use: N. Kaltsoyannis, *Dalton Trans.*, 2016, DOI: 10.1039/C5DT04317D.

ROYAL SOCIETY OF CHEMISTRY

www.rsc.org/dalton

Covalency hinders $AnO_2(H_2O)^+ \rightarrow AnO(OH)_2^+$ isomerisation (An = Pa–Pu)

View Article Online
DOI: 10.1039/C5DT04317D

Nikolas Kaltsoyannis

School of Chemistry, The University of Manchester, Oxford Road, Manchester M13 9PL, UK

nikolas.kaltsoyannis@manchester.ac.uk

Table of Contents Entry

Computational analysis of the electronic structures of $AnO_2(H_2O)^+$ (An = Pa–Pu) demonstrates that isomerisation to $AnO(OH)_2^+$ is least favoured for the system with the most covalent An–O_{yl} bond.

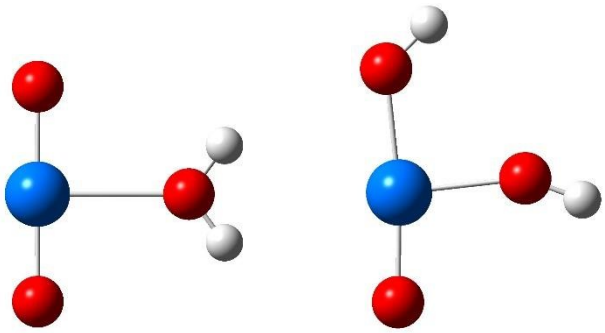

Abstract

The enthalpies of the reactions $AnO_2^+ \rightarrow AnO^+ + O$ and $AnO_2^+ + H_2O \rightarrow AnO_2(H_2O)^+$, and those of the isomerisation of the latter to $AnO(OH)_2^+$, have been calculated for An = Pa–Pu. The data match previous experimental and computational values very closely, and the computed enthalpy for the isomerisation of $PaO_2(H_2O)^+$ to $PaO(OH)_2^+$, requested by the authors of *Inorg. Chem.* 2015, **54**, 7474, is found to be 0.8 kJ/mol. The NPA, NBO and QTAIM approaches are used to probe covalency in the An–O_{yl} bond of $AnO_2(H_2O)^+$, and all metrics agree that these bonds become increasingly covalent as the 5f series is crossed, providing rationalisation for the increasingly endothermic isomerisation reactions. QTAIM analysis indicates that the An=O and An–OH bonds in the oxide hydroxide isomers also become increasingly covalent as the 5f series is crossed.

View Article Online
DOI: 10.1039/C5DT04317D

Introduction

One of the most lively and interesting debates in actinide chemistry in recent years centres on the nature and extent of covalency. For recent reviews, see references 1 and 2. Computational studies find increasingly large 5f contributions to what are expected to be mainly ligand-localised valence molecular orbitals as the series is crossed towards Am and Cm,[3, 4] appearing to contradict the traditional view of actinide chemistry,[5] which holds that as the series is crossed the elements display increasingly lanthanide-like, ionic behaviour. The reconciliation lies in the behaviour of the 5f orbitals across the actinide series; they become energetically stabilized and radially more contracted. Thus, at a certain point (dependent on the metal and the supporting ligand set) the 5f orbitals become degenerate with the highest lying ligand-based functions, yet are too contracted for there to be significant spatial overlap, leading to large metal/ligand atomic orbital mixings but little spatial overlap. We must therefore distinguish between *energy-driven* covalency (arising from the near degeneracy of metal and ligand orbitals) and the more traditional *overlap-driven* covalency; both types of covalency may be operative for different classes of complexes depending on the oxidation state and nature of the ligand.

Arguing that energy-driven covalency will not lead to a significant build-up of electron density in the internuclear region, my group introduced the Quantum Theory of Atoms-in-Molecules (QTAIM)[6, 7] as a tool for analyzing 5f molecular electron densities. Our first extensive use of this technique targeted $AnCp_4$[8] and $AnCp_3$,[9] ($Cp = \eta^5\text{-}C_5H_5$) and clearly demonstrated that while the largest 5f/Cp orbital mixings occur in systems toward the centre of the actinide series, these compounds also feature the lowest bond critical point (BCP) electron densities. These studies also showed that all of the An–C bonds are rather ionic, certainly on the basis of QTAIM definitions based on molecules much further up the periodic table, and that the least ionic bonds are found in the uranium systems. The uranium–ligand bond was also found to be the least ionic in our subsequent QTAIM studies of $An(^{Ar}acnac)_4$ (An = Th, U, Np, Pu; $^{Ar}acnac$ = Ar*N*C(Ph)CHC(Ph)*O*; Ar = 3,5-$^tBu_2C_6H_3$),[10] and diselenophosphinate complexes of Th–Pu.[11]

DOI: 10.1039/C5DT04317D

Elegant recent experimental work from Gibson *et al.* has targetted the gas phase reactions of AnO_2^+ (An = Pa–Pu) with water, and the subsequent isomerisation reactions of $AnO_2(H_2O)^+$ to $AnO(OH)_2^+$.[12, 13] A trend was observed toward increasingly endothermic isomerisations as the 5f series is crossed. This was rationalised on the basis of increasing covalency in the An–O_{yl} bond, which leads to larger barriers to disruption of the linear $\{O_{yl}–An–O_{yl}\}^+$ unit, though quantum chemical analysis of UO_2^+ and PuO_2^+ did not "definitively demonstrate" this.[12] Intrigued by this discussion, I here report recalculation of the potential surfaces for the isomerisation of $AnO_2(H_2O)^+$ to $AnO(OH)_2^+$ (An = U–Pu) using scalar relativistic, hybrid density functional theory (DFT), and also present that for $PaO_2(H_2O)^+$. I also report analysis of the An–O_{yl} bonding in $AnO_2(H_2O)^+$ (An = Pa–Pu) using the Natural Population Analysis (NPA), Natural Bond Orbital (NBO) and QTAIM methods, and find clear evidence for increases in all the covalency metrics as the 5f series is crossed. The QTAIM also provides strong evidence for increases in the covalent character of the An=O and An–OH bonds in $AnO(OH)_2^+$ from protactinium to plutonium.

Computational Details

View Article Online
DOI: 10.1039/C5DT04317D

All DFT calculations were performed with the Gaussian 09 code, revision D.01.[14] (14s 13p 10d 8f 5g)/[10s 9p 5d 4f 3g] segmented valence basis sets with Stuttgart-Bonn variety relativistic pseudopotentials were used for the actinides,[15, 16] and the 6-311++G(d,p) basis set was employed for the other elements. The B3LYP[17] functional was used, in conjunction with the ultrafine integration grid. The standard SCF convergence criterion (10^{-8}) was used.

All geometry optimisations were performed without symmetry constraints, and the geometry convergence criteria were tightened from the default *via* IOP(6/7=67), which produces 10^{-4} au for the maximum force. The resulting structures were verified as true minima or transition states *via* harmonic vibrational frequency analysis, and the connectivities of the transition states to neighbouring true minimum energy structures were verified by intrinsic reaction coordinate calculations.

All actinide species considered (bar AnO^+) feature the metal in the +5 oxidation state, corresponding to formal f electron counts of 0, 1, 2 and 3 respectively for Pa–Pu. For AnO^+ the actinide is in the +3 oxidation state, and the f electron counts are 2, 3, 4 and 5 respectively for Pa–Pu. Open-shell systems were studied in their high-spin ground states, and all converged electronic structures were subject to wavefunction stability checks *via* the stable=opt keyword, which sometimes resulted in lower total energies. These new electronic structures were fed into re-optimisations of the geometry.

QTAIM analyses were performed using the AIMALL program package,[18] with .wfx files generated in Gaussian 09 used as input. NBO analyses were performed with the NBO6 code,[19] interfaced with Gaussian 09.

Cartesian atomic coordinates and total energies of all converged structures are collected in the electronic supplementary information, as are (Table S1) the expectation values of the S^2 operator; there is little spin contamination in any of the systems studied.

Results and Discussion

View Article Online
DOI: 10.1039/C5DT04317D

The calculated enthalpies of reaction (1) for An = Pa–Pu are given in Table 1, together with the values recommended by Marçalo and Gibson.[20] Agreement is excellent, with only the computed value for UO_2^+ lying outside the literature error bars.[¥] The trend across the 5f series is pronounced, with the reaction becoming markedly less endothermic from PaO_2^+ to PuO_2^+.

$$AnO_2^+ \rightarrow AnO^+ + O \quad (1)$$

The computed enthalpies of reaction of AnO_2^+ with water are given in Figure 1. The reaction is in all cases significantly exothermic, very slightly more so for PaO_2^+ than the three heavier actinides. Using very similar methodology to that employed by Rios *et al.*,[12] and building on their work, I have recomputed the potential surfaces for the isomerisation of $AnO_2(H_2O)^+$ to $AnO(OH)_2^+$ (An = U, Np, Pu), and also calculated that for the $PaO_2(H_2O)^+$ isomerisation. These surfaces are also shown on Figure 1, and Figure 2 presents key structural data. In all four cases, the isomerisation proceeds *via* a transition state which transfers a hydrogen atom from the water to one of the yl oxygens. For An = U, Np and Pu, this transition state connects to $AnO(OH)_2^+$ in an essentially planar, T-shaped geometry. By contrast, and as noted by Dau *et al.*[13] and established originally by Siboulet *et al.*,[21] the structure of $PaO(OH)_2^+$ to which the transition state leads is slightly pyramidal.

The enthalpies of the isomerisation can be inferred from Figure 1 and are, respectively, 0.8, 52.5, 86.7 and 117.7 kJ/mol for Pa–Pu. As noted in references 12 and 13, isomerisation is increasingly endothermic from $UO_2(H_2O)^+$ to $PuO_2(H_2O)^+$, and the present data match the literature values very closely. Dau *et al.* conclude, from their very recent experimental study, that the isomerisation reaction

[¥] Such good agreement between experiment and theory is probably fortuitous for this reaction. Spin-orbit coupling is not considered and the spectroscopic state of the oxygen atom is not well defined in Gaussian. Nevertheless, the latter is the same for all four reactions and the data in Table 1 clearly show that, at the very least, the trend from PaO_2^+ to PuO_2^+ is well reproduced at the current computational level.

$PaO_2(H_2O)^+ \rightarrow PaO(OH)_2^+$ is "nearly thermoneutral, to within ca. 10 kJ/mol", and comment that "it would certainly be desirable to have a computed value [for this reaction]". I am pleased to provide this; the reaction is indeed essentially thermoneutral.

Vasiliu *et al.* have also very recently studied the reactions of water with PaO_2^+ and UO_2^+.[22] Using rather more sophisticated methodology than DFT (CCSD(T) extrapolated to the complete basis set limit with additional corrections including both scalar and spin-orbit relativistic effects) they obtain 0.4 kJ/mol and 49.0 kJ/mol respectively for the isomerisation reactions. Such good agreement with the present data suggests that DFT is capturing the essential features of this chemistry rather well.

As noted in references 12 and 13, and confirmed here, the activation of the $An–O_{yl}$ bond occurs much more readily for the earlier members of the series Pa–Pu, despite the data in Table 1. It was argued that this arises from greater covalency in the $An–O_{yl}$ bond as the series is crossed, which leads to an increasingly large barrier to disruption of the linear $\{O_{yl}–An–O_{yl}\}^+$ unit. However, the quantum chemical analysis of UO_2^+ and PuO_2^+ presented in reference 12 did "not definitively demonstrate a difference in covalency" (although it was "inferred….from the experimental observations"). I have therefore probed the $An–O_{yl}$ bond in $AnO_2(H_2O)^+$ (An = Pa–Pu) using the NPA, NBO and QTAIM methods; key data are collected in Table 2.

All of the metrics presented in Table 2 are well-established means to quantify covalency in the actinide series. The difference from the atomic 5f population expected for An(V) is a measure of the extent to which the 5f orbitals are involved in covalent bonding with the surrounding atoms; clearly this number increases steadily from Pa–Pu. The present data for $UO_2(H_2O)^+$, $NpO_2(H_2O)^+$ and $PuO_2(H_2O)^+$ are very similar to those computed previously for AnO_2^+ (An = U–Pu).[12] In agreement with this, the overall actinide contribution to the $An–O_{yl}$ π bonding NBOs[¶] increases by c. 30% from

[¶] I have chosen to present the composition data for the π bonds because they vary more consistently across the series than do the data for the σ NBOs, allowing for better comparisons between systems.

protactinium to plutonium (in all cases there is an almost exactly equal split between the 5f and 6d character of the π NBOs). Next come two QTAIM BCP metrics, the electron (ρ) and energy (H) densities.[7] Both of these are in all cases indicative of very covalent bonds, and both increase, in an absolute sense, from protactinium to plutonium. As with the 5f populations, the present ρ data for $UO_2(H_2O)^+$ and $PuO_2(H_2O)^+$ are very similar to those computed previously for UO_2^+ and PuO_2^+;[12] the latter are slightly larger due to the absence of coordinated water. The delocalisation index (DI) is a QTAIM measure of bond order, and again this increases toward the heavier actinides. The final row of data are the differences in QTAIM atomic partial charges between the actinide and the yl oxygen; this reduces from protactinium to plutonium, suggesting a less ionic bond.

Figure 3 reveals some remarkable correlations between these metrics, albeit with only four data points in each case. On all four graphs, there is essentially perfect linear correlation between the contribution of the actinide valence atomic orbitals to the An–O_{yl} π bond and the other measures of covalency (the correlation with H – not shown – is poorer (R^2 = 0.714), as a result of the datum for $NpO_2(H_2O)^+$). In my view, these data strongly support the argument that there is increasing covalency in the An–O_{yl} bonds from $PaO_2(H_2O)^+$ to $PuO_2(H_2O)^+$, and that the isomerisation barrier heights shown in Figure 1 most likely arise from the need to disrupt this increasingly covalent bonding.

It would thus appear that for the An–O_{yl} bonds in $AnO_2(H_2O)^+$, the covalency metrics based on orbital mixing, and those derived from the QTAIM, are in agreement in predicting increased covalency in the heavier actinides. This is in marked contrast to many of the other systems my group has studied *via* this combination of techniques, for which, as noted in the Introduction, the orbital mixing metrics suggest enhanced covalency across the series while the QTAIM indicates the opposite.[2, 8-11] It is likely that the present agreement of the orbital composition and electron density-based tools stems from the very short bonds under study; the ligating O_{yl} atoms are very close

In addition, the π bonds should be more sensitive to internuclear separation - and hence disruption of the $\{O_{yl}–An–O_{yl}\}^+$ moiety - than the σ.

to the actinide and the latter's valence functions overlap significantly with the oxygen 2p functions not only in energy, but also spatially.

View Article Online
DOI: 10.1039/C5DT04317D

Dau *et al.* suggest that the change in geometry from $PaO(OH)_2^+$ to $AnO(OH)_2^+$ (An = U–Pu) reflects an increase in covalency of the An–OH bond.[13] Table 3 presents QTAIM data for the An=O and An–OH bonds in $AnO(OH)_2^+$. ρ for the An=O bonds are almost identical to those for $An–O_{yl}$ in the water adduct, while the *H* values are generally a little smaller. By contrast, the DIs are slightly larger in the oxide hydroxide systems, by c. 0.1 in all cases. All three QTAIM metrics increase steadily from protactinium to plutonium, with the exception of *H*, which is smaller for Pu=O than Np=O. The QTAIM metrics for the An–OH bonds are all smaller, in an absolute sense, that those for An=O, reflecting the significantly longer actinide–oxygen bonds, but, importantly, all three steadily increase in magnitude from $PaO(OH)_2^+$ to $PuO(OH)_2^+$. Hence the QTAIM data support Dau *et al.*'s suggestion, and are in keeping with the trends in $An–O_{yl}$ covalency discussed above for the water adducts.

Conclusions

The enthalpies of the reactions $AnO_2^+ \rightarrow AnO^+ + O$ and $AnO_2^+ + H_2O \rightarrow AnO_2(H_2O)^+$, and the isomerisation of the latter to $AnO(OH)_2^+$, have been calculated for An = Pa–Pu. The data match previous experimental and computational values very closely; in particular, the enthalpy for the isomerisation of $PaO_2(H_2O)^+$ - characterised experimentally as "nearly thermoneutral"[13] – is pleasingly found to be 0.8 kJ/mol.

In order to explore the suggestion that the trend toward increasingly endothermic isomerisation as the 5f series is crossed arises from increasing covalency in the $\{O_{yl}–An–O_{yl}\}^+$ moiety, the $An–O_{yl}$ bonds have been probed using the NPA, NBO and QTAIM approaches. By contrast to previous study of the bonding in a subset of related compounds,[12] clear evidence is found from all the methods employed of increasingly covalency from protactinium to plutonium. The unusual agreement between the orbital composition- and QTAIM-based covalency metrics is traced to the short $An–O_{yl}$ distance.

The An=O and An–OH bonds in the oxide hydroxide isomers are also found to become increasingly covalent from protactinium to plutonium.

Acknowledgements

I am grateful for computational resources from the University of Manchester's Computational Shared Facility, and to the reviewers for their helpful comments.

View Article Online
DOI: 10.1039/C5DT04317D

Table 1: Enthalpy (kJ/mol, 298.15 K) of reaction (1).

Pa	U	Np	Pu	
790.7	695.2	618.5	528.0	This work
780 ± 29	741 ± 14	610 ± 22	509 ± 38	Data from reference 20

Table 2: NPA, NBO and QTAIM covalency metrics for the An–O_{yl} bond in $AnO_2(H_2O)^+$ (An = Pa–Pu). Data in parentheses for AnO_2^+ from reference 12.

Covalency metric	Pa	U	Np	Pu
Difference from the formal An 5f population	1.78	1.94 (1.98)	2.11 (2.15)	2.28 (2.31)
An contribution to An-O_{yl} π NBO (%)	17.6	19.4	21.2	22.9
ρ An–O_{yl} BCP (au)	0.302	0.312 (0.314)	0.318	0.328 (0.334)
H An–O_{yl} BCP (au)	-0.296	-0.303	-0.301	-0.320
An–O_{yl} DI	1.971	2.032	2.076	2.126
ΔQ_{QTAIM}(An/O_{yl})	3.775	3.532	3.307	3.170

Table 3: QTAIM covalency metrics for the An=O and An–OH bonds in $AnO(OH)_2^+$ (An = Pa–Pu). An–OH data for An = U–Pu for the bond *trans* to An=O.

Covalency metric	Pa	U	Np	Pu
ρ An=O BCP (au)	0.298	0.312	0.326	0.327
ρ An–OH BCP (au)	0.140	0.152	0.166	0.173
H An=O BCP (au)	-0.285	-0.297	-0.310	-0.301
H An–OH BCP (au)	-0.055	-0.066	-0.079	-0.082
An=O DI	2.072	2.148	2.199	2.218
An–OH DI	1.130	1.173	1.230	1.252

Figure 1: Relative enthalpy (298.15 K, kJ/mol) surfaces for the isomerisation reactions $AnO_2(H_2O)^+ \rightarrow AnO(OH)_2^+$ (An = Pa–Pu). Line/number colours: black – Pa, red – U, green – Np, blue – Pu. Atom colours: blue – actinide, red – O, white – H.

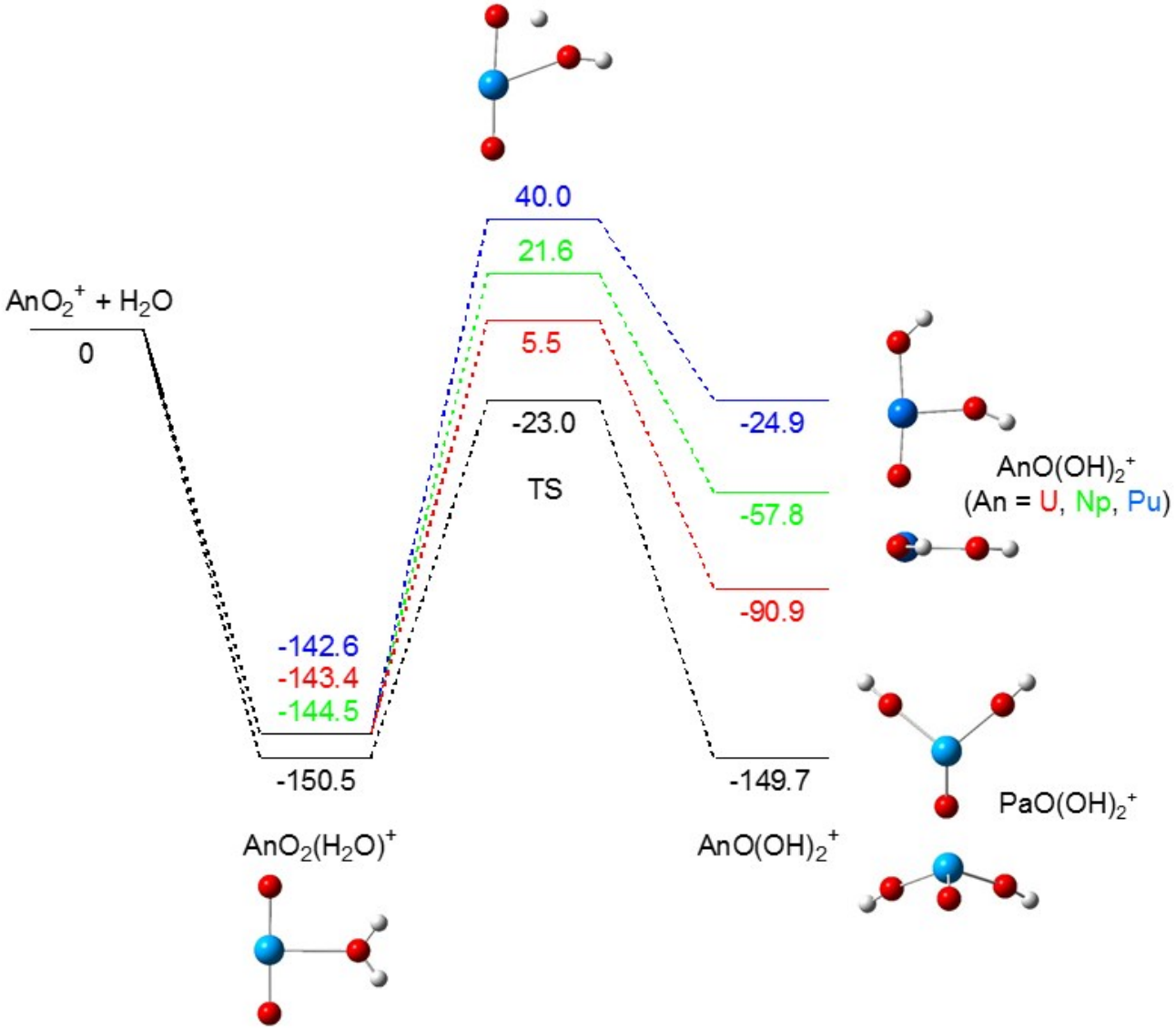

Figure 2: Geometric data for the stationary points in the isomerisation $AnO_2(H_2O)^+ \rightarrow AnO(OH)_2^+$ (An = Pa–Pu). Number colours: black – Pa, red – U, green – Np, blue – Pu. Atom colours: blue – actinide, red – O, white – H. The dihedral angle O–Pa–O(H)–O(H) in $PaO(OH)_2^+$ is 121.8º, almost identical to that reported by Siboulet *et al.*[21]

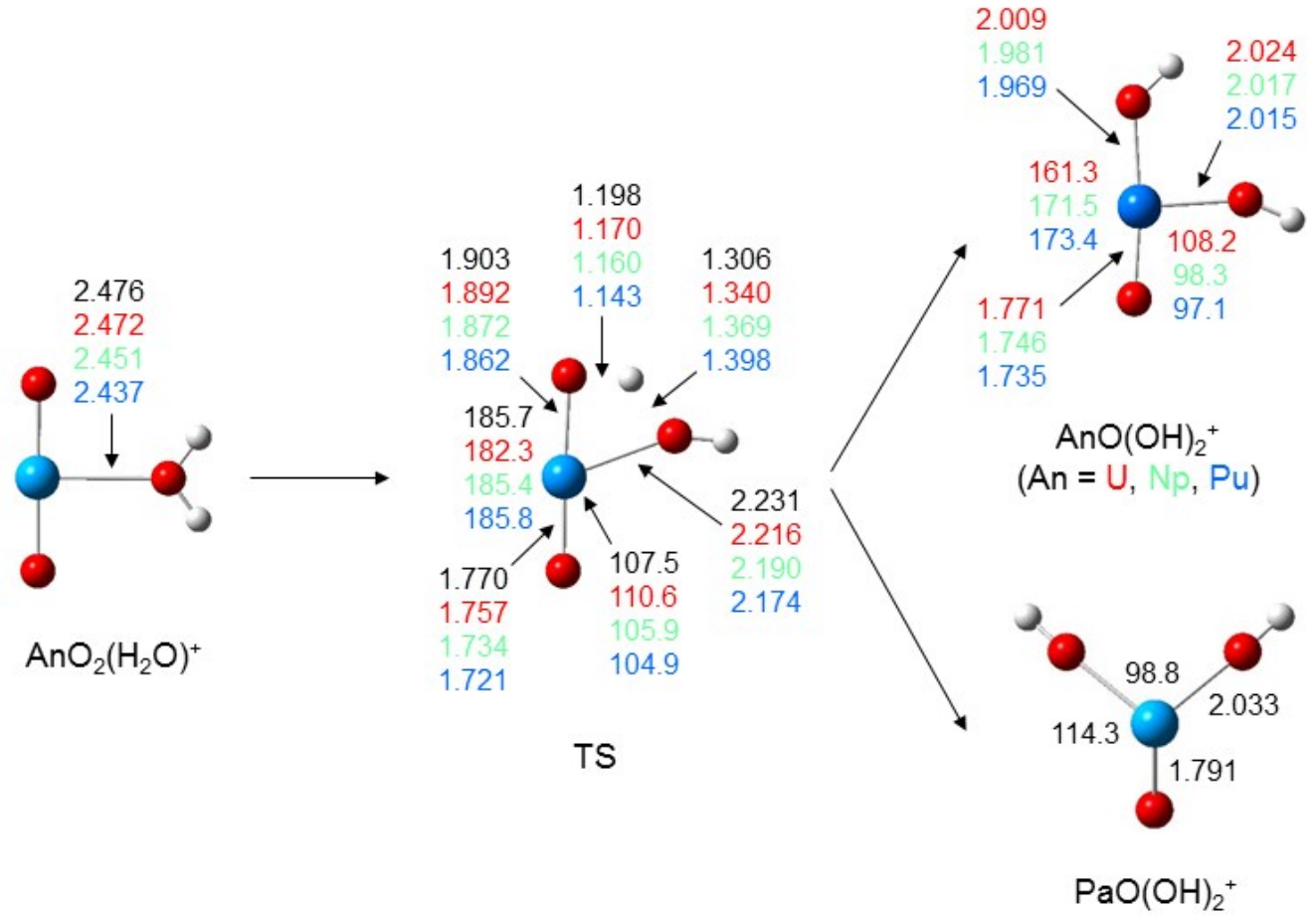

Figure 3: Correlations of the actinide contribution to the An–O_{yl} π NBOs with the (a) difference from the formal An 5f population (b) An–O_{yl} BCP ρ (c) An–O_{yl} delocalisation indices and (d) An/O_{yl} QTAIM charge difference. R^2 values are (a) 0.999 (b) 0.989 (c) 0.996 and (d) 0.988.

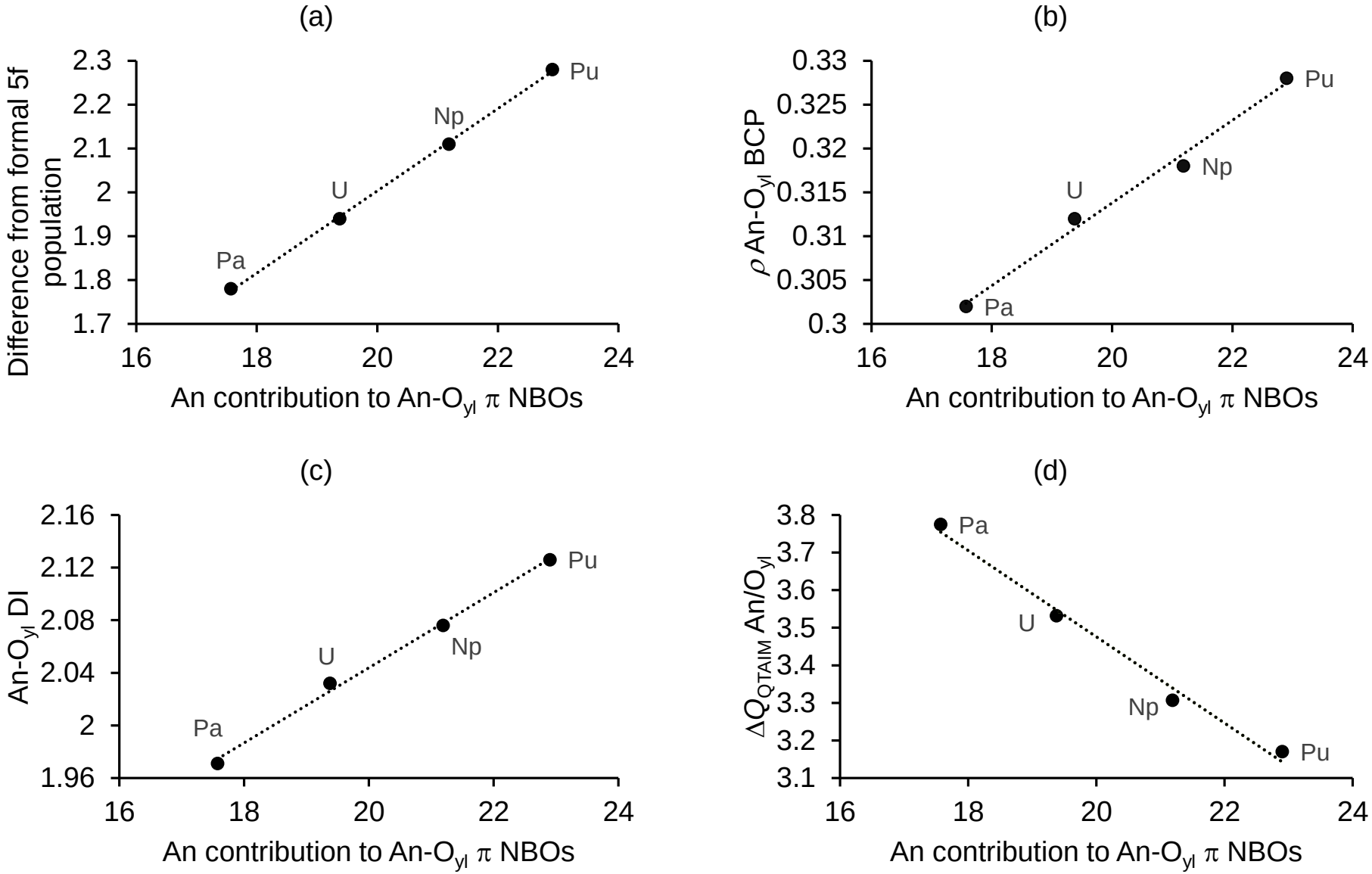

View Article Online
DOI: 10.1039/C5DT04317D

References

1. M. L. Neidig, D. L. Clark and R. L. Martin, *Coord. Chem. Rev.*, 2013, **257**, 394.
2. N. Kaltsoyannis, *Inorg. Chem.*, 2013, **52**, 3407.
3. R. J. Strittmatter and B. E. Bursten, *J. Am. Chem. Soc.*, 1991, **113**, 552.
4. K. I. M. Ingram, M. J. Tassell, A. J. Gaunt and N. Kaltsoyannis, *Inorg. Chem.*, 2008, **47**, 7824.
5. N. Kaltsoyannis and P. Scott, *The f elements*, Oxford University Press, Oxford, 1999.
6. R. F. W. Bader, *Atoms in Molecules: A Quantum Theory*, OUP, Oxford, 1990.
7. C. F. Matta and R. J. Boyd, in *The quantum theory of atoms in molecules*, eds. C. F. Matta and R. J. Boyd, Wiley-VCH, Weinheim, 2007, pp. 1-34.
8. M. J. Tassell and N. Kaltsoyannis, *Dalton Trans.*, 2010, **39**, 6719.
9. I. Kirker and N. Kaltsoyannis, *Dalton Trans.*, 2011, **40**, 124.
10. D. D. Schnaars, A. J. Gaunt, T. W. Hayton, M. B. Jones, I. Kirker, N. Kaltsoyannis, I. May, S. D. Reilly, B. L. Scott and G. Wu, *Inorg. Chem.*, 2012, **51**, 8557.
11. M. B. Jones, A. J. Gaunt, J. C. Gordon, N. Kaltsoyannis, M. P. Neu and B. L. Scott, *Chem. Sci.*, 2013, **4**, 1189.
12. D. Rios, M. d. C. Micheini, A. F. Lucena, J. Marcalo and J. K. Gibson, *J. Am. Chem. Soc.*, 2012, **134**, 15488.
13. P. D. Dau, R. E. Wilson and J. K. Gibson, *Inorg. Chem.It clearly demonstrates* , 2015, **54**, 7474.
14. M. J. Frisch, G. W. Trucks, H. B. Schlegel, G. E. Scuseria, M. A. Robb, J. R. Cheeseman, G. Scalmani, V. Barone, B. Mennucci, G. A. Petersson, H. Nakatsuji, M. Caricato, X. Li, H. P. Hratchian, A. F. Izmaylov, J. Bloino, G. Zheng, J. L. Sonnenberg, M. Hada, M. Ehara, K. Toyota, R. Fukuda, J. Hasegawa, M. Ishida, T. Nakajima, Y. Honda, O. Kitao, H. Nakai, T. Vreven, J. Montgomery, J. A., J. E. Peralta, F. Ogliaro, M. Bearpark, J. J. Heyd, E. Brothers, K. N. Kudin, V. N. Staroverov, R. Kobayashi, J. Normand, K. Raghavachari, A. Rendell, J. C. Burant, S. S. Iyengar, J. Tomasi, M. Cossi, M. Rega, N. J. Millam, M. Klene, J. E. Knox,

View Article Online
DOI: 10.1039/C5DT04317D

J. B. Cross, V. Bakken, C. Adamo, J. Jaramillo, R. E. Gomperts, O. Stratmann, A. J. Yazyev, R. Austin, C. Cammi, J. W. Pomelli, R. Ochterski, R. L. Martin, K. Morokuma, V. G. Zakrzewski, G. A. Voth, P. Salvador, J. J. Dannenberg, S. Dapprich, A. D. Daniels, O. Farkas, J. B. Foresman, J. V. Ortiz, J. Cioslowski and D. J. Fox, Gaussian 09 revision D.01, Gaussian Inc., Wallingford CT, 2009.

15. X. Y. Cao and M. Dolg, *J. Mol. Struct. (TheoChem)*, 2004, **673**, 203.

16. X. Y. Cao, M. Dolg and H. Stoll, *J. Chem. Phys.*, 2003, **118**, 487.

17. A. Becke, *Phys. Rev. A.*, 1988, **38**, 3098.

18. T. A. Keith, AIMAll v 15.05.18, http://aim.tkgristmill.com/, 2015.

19. E. D. Glendening, J. K. Badenhoop, A. E. Reed, J. E. Carpenter, J. A. Bohmann, C. M. Morales, C. R. Landis and F. Weinhold, NBO6.0, http://nbo6.chem.wisc.edu/, 2013.

20. J. Marcalo and J. K. Gibson, *J. Phys. Chem. A*, 2009, **113**, 12599.

21. B. Siboulet, C. J. Marsden and P. Vitorge, *N. J. Chem.*, 2008, **32**, 2080.

22. M. Vasiliu, K. A. Peterson, J. K. Gibson and D. A. Dixon, *J. Phys. Chem. A*, 2015, **119**, 11422.